J. Mol. Model. **1997**, *3*, 224 – 232

Molecular Dynamics Simulations of Zinc Ions in Water Using CHARMM[$]

Stefan Obst* and Hans Bradaczek

Freie Universität Berlin, Fachbereich Chemie, Institut für Kristallographie, Takustr. 6, D-14195 Berlin, Germany; Tel.: +49-30-838 3457; Fax: +49-30-838 3464 (obst@chemie.fu-berlin.de)

Received: 13 June 1997 / Accepted: 24 June 1997 / Published: 30 June 1997

Abstract

Molecular Dynamics simulations of a zinc ion with 123 and 525 TIP3P-water molecules were carried out with CHARMM using two different Lennard-Jones parameter sets for the Zn^{2+} ion. The results were compared to published experimental and simulation data. Good agreement was found for radial distribution functions, number of hydrogen bonds, and diffusion coefficients. Experimental radial distribution functions were better reproduced by the original CHARMM22 parameter set than by the parameter set modified by Stote and Karplus. Diffusion coefficients were found to depend on the system size rather than on the parameter set used and were better reproduced by the larger systems. The divalent zinc ion exerts a strong influence on its hydration shell as indicated by the high first peak of the radial distribution function. Water molecules in the vicinity of the zinc ion show a slight deformation of the O-H bond length and of the H-O-H bond angle as compared to pure water. No water molecules from the first hydration shell were exchanged during 1 ns of MD simulation.

Keywords: molecular dynamics simulation, charmm, zinc, water

Introduction

Zinc is the second most abundant inorganic metal cation in biological systems and it can be found in many proteins. Either structural and/or catalytic roles are proposed for zinc ions in proteins [1]. Zinc plays a structural role in zinc finger domains (e.g. transcription factor IIIA) and in metallothioneins for example. It is part of the active site of enzymes like carbonic anhydrase, carboxypeptidase A, and alkaline phosphatase to name a few. An extensive review on zinc enzymology was recently given by Lipscomb and Sträter [2].

Compared to other metal ions of biological importance like Ca^{2+}, Mg^{2+}, or Fe^{3+}, which are hard cations, Zn^{2+} is a borderline cation whereas Cu^{+} and Cd^{2+} are soft cations. This has implications for the choice of ligands and for the preferred architecture of the coordination sphere. Being a d^{10} metal ion, Zn^{2+} is not subjected to ligand field stabilisation effects. In consequence, a number of different coordination geometries are almost equally favourable for the Zn^{2+} ion as was proven by ab initio calculations [3]. Whereas in water hexa-coordinated species dominate over tetra and penta-water complexes, in proteins tetrahedral complexes are most frequent[1]. A large number of experimental studies dealing with the structure and dynamics of the hydration shell of

[$] *Presented at the 11. Molecular Modeling Workshop, 6 -7 May 1997, Darmstadt, Germany*

* *To whom correspondence should be addressed*

Table 1. *Parameters for potential functions used in the calculations. q: atomic charge; E_{min}, r_{min}: parameters for the calculation of the Lennard-Jones potential. O, H: TIP3P water model [23]; Zn (CHARMM): CHARMM22 force field as supplied by MSI; Zn(Stote/Karplus): parameters from Stote and Karplus [20].*

	O	H	Zn [a]	Zn [b]
q	-0.834	0.417	2	2
E_{min} (kcal/mol)	-0.1521	-0.0498	-0.250	-0.250
r_{min} (Å)	1.768	0.920	1.090	0.975

[a] CHARMM
[b] Stote/Karplus

zinc have been carried out in the past. X-ray diffraction [4, 5, 6, 7], neutron scattering [8, 9], EXAFS [10] and NMR techniques[11, 12] were employed for the investigation of the structure of the hydration shell. The dynamics of the hydration shell was investigated by quasi-elastic neutron scattering [13]. Much of this work has been reviewed by Ohtaki and Radnai [14], Johannson [15] and Marcus [16]. The hydration of zinc ions was compared to Mg^{2+} and Be^{2+} by ab initio calculations by Bock et al.[3] and Monte Carlo calculations of Zn^{2+}-water systems were carried out by Clementi et al. [17], Yongyai et al. [18] and Marchese et al.[19].

In 1995, Stote and Karplus [20] published a set of parameters for the simulation of zinc in water and in proteins which had been improved with regard to the interaction energy profile. This parameter set was based on the original CHARMM parameter set and on ab initio calculations by Clementi et al. [17]. The aim of the present work was to assess the differences in the structure and dynamics of the hydration shell of zinc between these two parameter sets and to compare them to experimental data.

Methods

Molecular dynamics calculation were carried out using CHARMM [21] (V. 24g1) on SGI computers (Origin 2000 and Octane). Two different parameter sets were used:
(1) the CHARMM22 force field as supplied by MSI (Molecular Simulations Inc., Waltham, MA) and
(2) optimised parameters for the zinc-water Lennard-Jones potential published by Stote and Karplus [20].

The interaction parameters used for the calculations are given in Table 1.

The simulation was carried out as previously described [22]. In brief, a zinc ion was placed in the middle of a cubic box of TIP3P water molecules [23] and water molecules overlapping the Zn^{2+} ion were deleted. The resulting ensemble was energy minimised and then subjected to MD simulation. The simulation consisted of 10 ps heating phase from 0 to 300 K, 10 ps equilibration phase and 250 ps (1000 ps) simulation phase. 250 ps of the latter was used for subsequent data analysis. For comparison, pure water systems were simulated for 100 ps. Two different system sizes were used (cf. Table 2). The leapfrog integrator was used with a time step of 1 fs. Bonds involving hydrogens were controlled by SHAKE [24]. During the MD, coordinates and velocities were stored at every 100th time step, i.e. every 0.1 ps. Three-dimensional periodic boundary conditions were used [25]. Nonbonded interactions were cut off at 12 Å by the SHIFT function [21]. For electrostatic calculations $\varepsilon = 1$ was used.

Radial pair distribution function

The radial pair distribution function (RDF) $g_{X\text{-}O}(H)(r)$ between water oxygen O (hydrogen H) and a second atom X

Table 2. *System size and parameters used for the MD simulations. n(H_2O), n(Zn^{2+}): number of water molecules (zinc ions) in the simulation box; box size: length of the cubic simulation box; parameters: MSI: CHARMM22 parameter set as supplied by MSI, Stote/Karplus: modified parameters for the zinc ion [20]; t: duration of the simulation phase used for data analysis (excluding heating and equilibration phases of 10 ps each).*

simulation	n(H_2O)	n(Zn^{2+})	box size (Å)	parameter	t (ps)
Zn-123	123	1	15.50	MSI	1000
Zn-123-K	123	1	15.50	Stote/Karplus	250
Zn-525	525	1	25.08	MSI	1000
Zn-525-K	525	1	25.08	Stote/Karplus	250
H2O-125	125	0	15.50	MSI	100
H2O-528	528	0	25.08	MSI	100

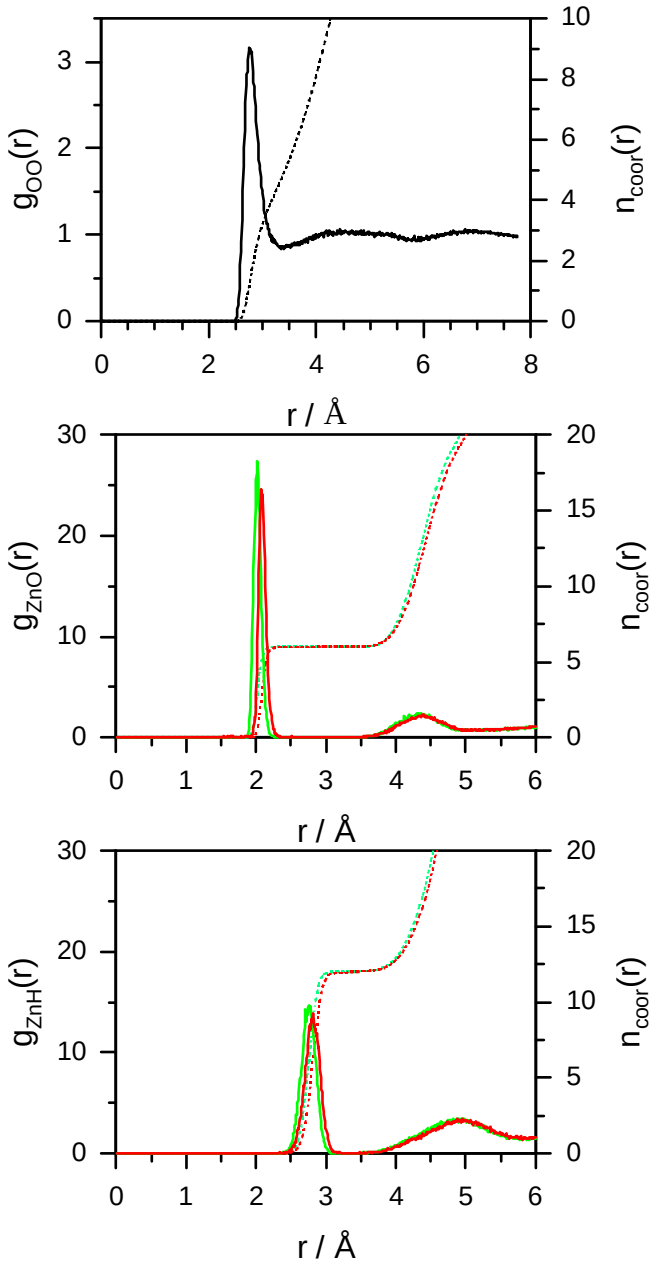

Figure 1. *Coordination numbers $n_{coor}(r)$ and radial distribution functions $g_{OO}(r)$ for pure water (top), and $g_{Zn\text{-}O}(r)$ (middle) and $g_{Zn\text{-}H}(r)$ (bottom) for solutions containing zinc. Red: CHARMM22 parameters; green: Stote/Karplus parameters; solid line: g(r); dotted line: $n_{coor}(r)$.*

was calculated for pure water (X = O) and zinc (X = Zn). By integration of $g(r)4\pi r^2dr$ from r = 0 up to $r = r_{1st\ min}$ the coordination number $n_{coor}(r)$ was calculated [25].

Average structure of the first hydration shell

The average structure of the first hydration shell of Zn^{2+} was calculated by least-squares fit (LSQ) of the water oxygen atoms using 10000 coordinate sets derived from the MD trajectory of 1 ns. The LSQ-fitted coordinates were centred on the zinc ion located at (0,0,0) and oriented on the axes of a Cartesian coordinate system with four oxygen atoms in the x-y plane and two oxygen atoms on the z-axis.

Water geometry

The geometry of the water molecules was analysed in terms of O-H bond length and of H-O-H bond angle. The monomer values for the TIP3P water model [23] are r_{OH} = 0.9572 Å and ∠(H-O-H) = 104.52°.

Hydrogen bonds

A geometric criterion was employed for the detection of hydrogen bonds: distance between the two water-oxygen atoms < 3.4 Å and O-H···O angle >135° [26, 27]. The fraction p of water molecules participating in a given number of hydrogen bonds (n(HB) = {0..5}) was analysed.

Diffusion coefficient

From mean square displacements (MSD) the diffusion coefficient D was calculated using the Einstein relation [28]:

$$D = \lim_{t\to\infty} \frac{\left\langle \left[z_i(t) - z_i(0) \right]^2 \right\rangle}{2t},$$

where $z_i(t)$ is the z-(x-, y-) coordinate of particle i at time t and $z_i(0)$ is the z-(x-, y-) coordinate of particle i at time t = 0. The MSD was calculated independently for segments of 5 ps duration and finally averaged. All D values are given in 10^{-5} cm^2/s.

Results and discussion

Radial pair distribution functions (RDF) were calculated for solutions containing zinc and for pure water. The results are shown in Figure 1 and peak positions are given in Table 3. No dependency of the RDFs on the system size was found, hence only RDFs for the larger systems are shown. Depending on the interaction potential used, the position of maxima and minima of the RDFs is slightly different. The first peaks of $g_{Zn\text{-}O}(r)$ and $g_{Zn\text{-}H}(r)$ are shifted 0.06 Å closer to the zinc ion when the Stote/Karplus parameters are used. This is accompanied by slightly higher peak values for these RDFs resulting from the fact that the coordination number remains constant independent from the interaction parameters used.

The RDF of pure water is in good agreement with experimental results as discussed elsewhere [22]. Two distinct hydration shells can be identified for pure water and for zinc. This confirms experimental [5, 6, 12, 14, 36] and theoretical

Table 3. *Minima and maxima of the radial distribution function g(r) and coordination numbers n_{coor} for Zn-O and Zn-H. Top: first shell; r_{OX}: distance between water oxygen and atom X (X = Zn^{2+} for solutions containing zinc and X = O for pure water); n_{coor}(O(H)): number of oxygen (hydrogen) atoms in the first hydration shell, calculated by integration of g(r) from r = 0 to r = $r_{1st\ min}$.*

1st shell	**oxygen**					**hydrogen**				
	1st max		**1st min**			**1st max**		**1st min**		
	r_{OX} (Å)	g_{OX}	r_{OX} (Å)	g_{OX}	n_{coor}(O)	r_{HZn} (Å)	g_{HZn}	r_{HZn} (Å)	g_{HZn}	n_{coor}(H)
H_2O-125	2.76	3.2	3.34	0.9	4.4					
Zn-525	2.07	24.7	2.35-3.44	0.0	6.0	2.82	13.9	3.14-3.54	0.0	12.0
Zn-525-K	2.01	27.4	2.31-3.47	0.0	6.0	2.76	14.7	3.09-3.50	0.0	12.0
$ZnCl_2$ [a]	2.09				4.1	2.74				8.2
$Zn(CF_3SO_3)_2$[b]	2.09				5.3	2.69				10.6
$Zn(SO_4)$ [c]	2.08				5.9					
$Zn(SO_4)$ [d]	2.13				6.0					

2nd shell	**oxygen**					**hydrogen**				
	2nd max		**2nd min**			**2nd max**		**2nd min**		
	r_{OX} (Å)	g_{OX}	r_{OX} (Å)	g_{OX}	n_{coor}(O)	r_{HZn} (Å)	g_{HZn}	r_{HZn} (Å)	g_{HZn}	n_{coor}(H)
H_2O-125	4.76	1.0	5.80	0.9	22					
Zn-525	4.39	2.1	4.93	0.7	14	5.0	3.2	5.9	1.5	43
Zn-525-K	4.35	2.3	4.88	0.7	14	4.9	3.3	5.8	1.5	43
$Zn(SO_4)$ [d]	4.26				12.5					

[a] neutron scattering [7]
[b] neutron scattering [36]
[c] X-ray diffraction [37]
[d] X-ray diffraction [5]. Bottom: second shell; r_{OX}: distance between water oxygen and atom X (X = Zn^{2+} for solutions containing zinc and X = O for pure water); n_{coor}(O(H)): number of oxygen (hydrogen) atoms in the second hydration shell, calculated by integration of g(r) from r = $r_{1st\ min}$ to r = $r_{2nd\ min}$; note that second shell peaks are less well defined than the structure of the first shell.

[17, 18] results suggesting the presence of a second hydration shell for zinc. A number of reviews [9, 15, 16] cite Zn-O distances ranging essentially from 2.05 to 2.17 Å with the exception of r_{ZnO} = 1.94 Å calculated from EXAFS experiments [10] using $ZnBr_2$ solutions. The hydration numbers range from 2.4 to 7.0 with most of the experiments yielding a coordination number of 6. Some experimental values are given in Table 3. From MC calculations, Yongyai et al. [18] derived RDFs with a sharp peak at r = 2.05 Å and a coordination number of 5.6. Ab initio calculations resulted in a Zn-O bondlength of 2.14 Å for $Zn[H_2O]_6^{2+}$ and the average Zn-O distance found in the Cambridge Structural Database (CSD) for hexahydrated zinc ions is 2.09 Å [3]. Although the exact value of the Zn-O distance seems to depend on the system investigated, the counterion involved and the experimental method used, the position of the first peak produced by the CHARMM22 parameter set is in better agreement with the majority of experimental results than the modified parameter set by Stote and Karplus. On the other hand, the Zn-H distance is better reproduced by the modified parameter set. This indicates a different orientation of the first shell water molecules in the simulation and the experiments. The so-called tilt angle of water molecules is defined by the bisector of the H-O-H angle of a water molecule and the Zn-O vector [29]. The difference between the positions of the first peak obtained for the two different parameter sets amounts only to approx. 50% of the difference between the r_{min} values of the two different Lennard Jones parameter sets. This is probably caused by repulsive forces between neighbouring water molecules.

The second hydration shell of both Zn^{2+} and pure water is blurred as compared to the first shell. Values defining the second shell are given at the bottom of Table 3. The position of the second hydration shell of Zn^{2+} at r = 4.3 - 4.4, as de-

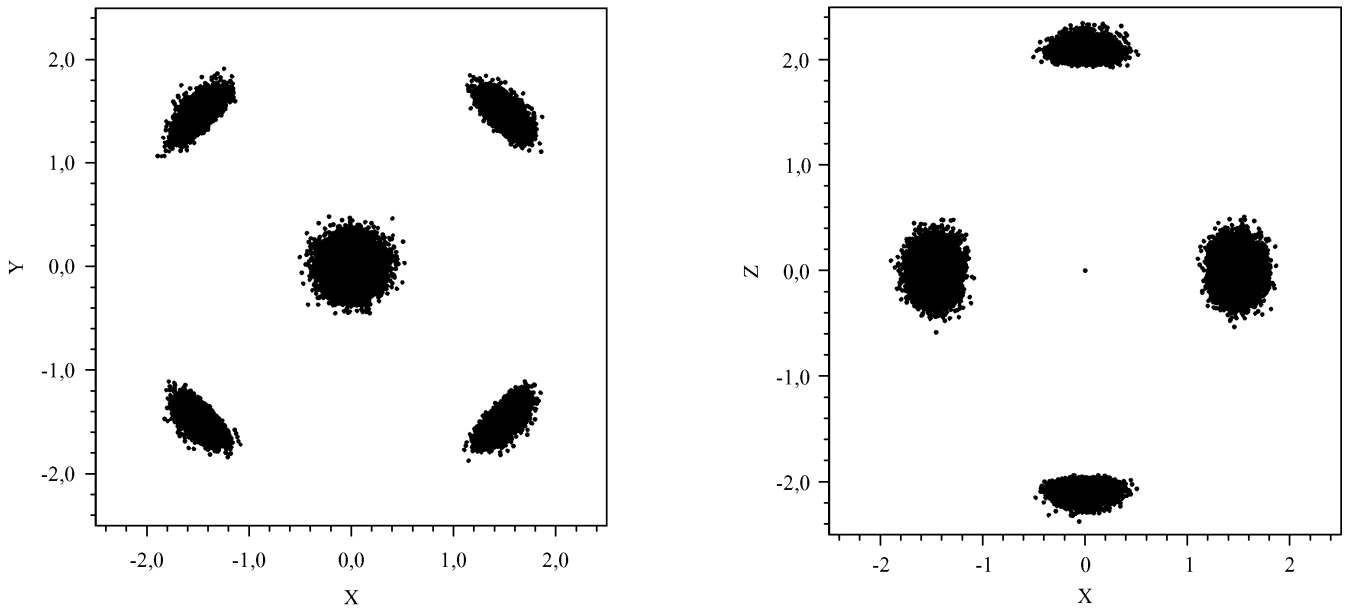

Figure 2. *Overlay plot of oxygen positions from 10000 conformations taken from simulation Zn-525 showing the average structure of the first hydration shell of zinc. Left: x-y plane; right: x-z plane. Zinc is located at (0, 0, 0).*

fined by the second peak of $g_{Zn\text{-}O}$, is slightly shifted to larger distances as compared to experimental results [14]. From an x-ray study of a highly concentrated solution of $Zn(NO_3)_2$, Dagnall et al. estimated the presence of 10.8 H_2O in the second shell at a distance of 4.1 Å [6]. Depending on the concentration of the $ZnSO_4$ solution investigated, Licheri et al. reported 7.3 to 13.2 water molecules in the second hydration shell at distances between 4.21 and 4.26 Å [5].

The number of approx. 43 hydrogens in the second hydration shell of zinc is significantly higher than twice the number of 14 oxygens found in the second hydration shell, whereas in the first shell, for each oxygen exactly two hydrogens can be found. The increased number of hydrogens found in the second shell indicates the decrease of order with increasing distance from the zinc ion. If each hydrogen of the six water molecules in the first shell was hydrogen bonded to one water molecule in the second hydration shell, then 12 oxygens would be found in the second hydration shell. This is close to values reported for Fe^{2+} (13 H_2O) and Li^+ (14 H_2O) determined by MC calculations [30]. Two MC studies of zinc solutions reported 16 to 18 water molecules in the second hydration shell of Zn^{2+} [17, 18]. Taking into account the uncertainty arising from shallow second peaks of the RDF, our results are in good agreement with these data. The increased number of hydrogens in the second shell presumably results from hydrogens bound to oxygens not belonging to the first or second hydration shell, i.e. some water molecules (of the bulk) are oriented with their hydrogens towards the zinc ion, which is not found for water molecules in the first or second hydration shell.

In Figure 2, the average structure of the hydration shell of Zn-525 is depicted. The oxygen atoms are located octahedrally in spherical segments with small deviation of the Zn-O distance but with increased flexibility of the O-Zn-O angle. The coordinates (± standard deviation sd) resulting from the fit procedure do not vary with the system size and are given for Zn-125 and Zn-125-K in Table 4. Note that for oxygens 3 and 6 the standard deviation of the y-component (i.e. in the direction of the Zn-O bond) of its position vector is half the value obtained for the standard deviation of the x-

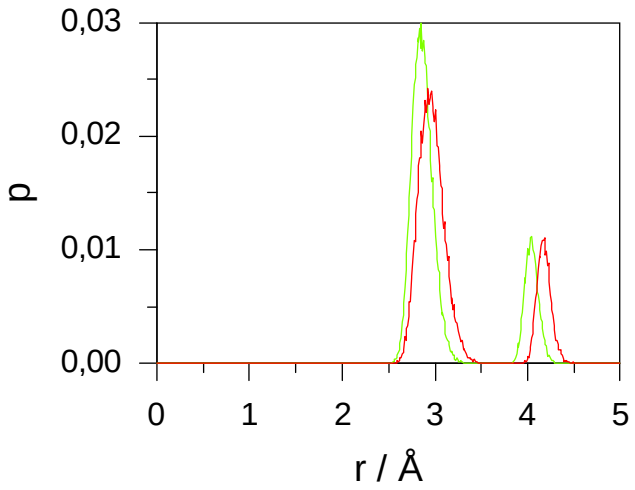

Figure 3. *Distribution of O-O distances of water molecules of the first hydration shell of zinc. Red: CHARMM22 parameters; green: Stote/Karplus parameters.*

Table 4. *Average coordinates of oxygen atoms from the first hydration shell of zinc calculated from 250 ps MD simulation with CHARMM-parameters (top) and Stote/Karplus-parameters (bottom). The numbering of oxygen atoms is arbitrary.*

oxygen	x (Å)	± sd	y (Å)	± sd	z (Å)	± sd
1	-1.48	0.10	0.00	0.12	1.48	0.10
2	-1.48	0.10	0.00	0.13	-1.47	0.09
3	0.00	0.12	-2.09	0.05	0.00	0.12
4	1.48	0.09	0.00	0.12	-1.47	0.09
5	1.48	0.09	0.00	0.12	1.48	0.10
6	0.00	0.12	2.09	0.06	0.00	0.12

oxygen	x (Å)	± sd	y (Å)	± sd	z (Å)	± sd
1	-1.43	0.08	0.00	0.10	1.44	0.08
2	-1.43	0.08	0.00	0.10	-1.42	0.08
3	0.00	0.10	-2.02	0.06	0.00	0.10
4	1.43	0.08	0.01	0.10	-1.42	0.08
5	1.42	0.08	0.00	0.10	1.44	0.08
6	0.00	0.10	2.02	0.05	0.00	0.10

and z-components. This observation is in good agreement with the calculations of Marchese and Beveridge [19] who plotted thermal ellipsoids for the water molecules in the first hydration shell of zinc from a MC simulation. They concluded that the strength of the ion-water potential minimised the radial motions but allowed for twisting and bending motions of the hydrating water molecules.

In Figure 3, the O-O distances in the first hydration shell of zinc are shown. As discussed above, the Stote/Karplus parameters lead to decreased Zn-O distances and hence to decreased O-O distances in the first shell. The distribution of distances is broader for the CHARMM22 parameters in the case of the O-O distances of neighbouring oxygen atoms whereas for the O-Zn-O distances, the distribution has a comparable width. The latter is controlled by the Zn-O interaction energy which is comparable for both parameter sets. The former on the other hand depends mainly on the uncertainty of the oxygen position which increases with increasing distance from the zinc ion.

In Figure 4, the distribution of O-Zn-O angles in the first hydration shell is shown. Again, the distribution is wider for the CHARMM22 parameter set and narrower for the Stote/Karplus parameters. As expected from the octahedral structure of the hydration shell, the first peak is centred at approx. 90°. The second peak, on the other hand, is centred at approx. 173°, i.e. the water molecules are arranged on a distorted octahedron. This can also be seen in Figure 5, where a representative snapshot taken from simulation Zn-123 shows zinc with its first hydration shell as a stereo plot.

As can be seen in Table 5, the average geometry of the water molecules computed from the MD trajectory deviated from the monomer parameters given in the Methods section. In the first shell, the O-H bond is lengthened by 1% as compared to pure or bulk water. At the same time, the first shell H-O-H bond angle is decreased by 1.6° to 2.8°. Pure water properties are found for water molecules not belonging to the first shell. By ab initio calculations of $Zn[H_2O]_6^{2+}$-clusters, Bock et al. [3] found H-O-H angles of 107.1° for first shell water molecules and of 105.5° for an isolated water molecule, which is in contrast to our results. This might in part be due to the fact that the ab initio calculations do not account for a second hydration shell of the zinc ion or the hydration of the single water molecule. In agreement with our observations, van der Maarel [31] noted an increase of the O-H bond length from 0.98 Å in pure water to 1.01 Å in a 17.2 M $ZnCl_2$ solution by NMR.

The fraction of water molecules participating in a given number of hydrogen bonds n(HB) is shown in Figure 6. The hydrogen bond distribution is not influenced by the parameter set used but the effect of the system size is clearly visible. In the small systems (Zn-123, Zn-123-K), the largest fraction of water molecules participates in two hydrogen bonds at the same time, whereas in bulk water (H_2O-125, H_2O-528) and in the large systems (Zn-525, Zn-525-K) the distribution is shifted towards higher n(HB). No influence of the presence of Zn^{2+} on the number of hydrogen bonds in the solution can be seen for the large systems, whereas for the small systems the presence of zinc leads to a small decrease

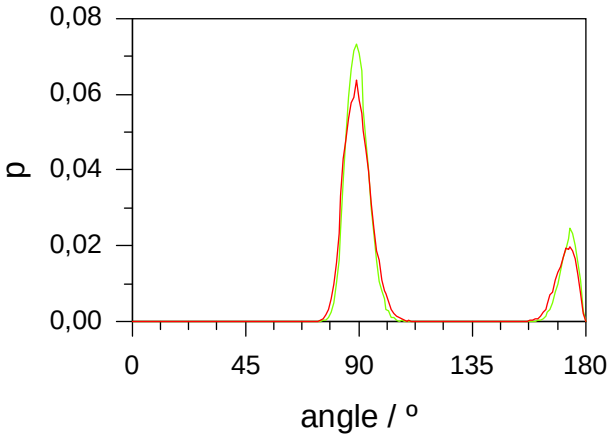

Figure 4. *Distribution of O-Zn-O angles in the first hydration shell of zinc. Red: CHARMM22 parameters; green: Stote/Karplus parameters.*

Table 5. *Average geometry of water molecules in the first hydration shell and in the bulk. 1st shell: all water molecules closer to the central particle (Zn^{2+} for Zn-123, Zn-123-K, Zn-525, and Zn525-K or water for H_2O-125) than $r_{first\ min}$ given in Table 3; bulk: all water molecules not belonging to the first shell. r_{O-H}: average O-H bond length; sd: standard deviation of r_{O-H}; ∠(H-O-H): average H-O-H bond angle of water molecules; sd: standard deviation of ∠(H-O-H).*

	1st shell		bulk		1st shell		bulk	
	r_{O-H} (Å)	sd	r_{O-H} (Å)	sd	∠(H-O-H) (°)	sd	∠(H-O-H) (°)	sd
H2O-125	0.980	0.005	0.980	0.005	101.1	1.1	100.7	1.2
Zn-123	0.989	0.005	0.980	0.006	98.0	1.1	100.2	0.2
Zn-123-K	0.989	0.005	0.980	0.005	97.9	1.1	100.3	1.4
Zn-525	0.99	0.02	0.99	0.06	99.5	1.8	99.1	5.0
Zn-525-K	0.989	0.006	0.979	0.006	98.3	1.3	100.3	1.4

in n(HB). This is presumably due to the fact that the influence of the solute exerted on the water molecules of the first hydration shell is outnumbered by the large number of water molecules unaffected by the solute in the case of the large system whereas in the small system, fewer uninfluenced water molecules are present. For bulk SPC water, Kowall and Geiger [27] found a distribution which was shifted to higher n(HB) as compared to our simulations. They give an average n_{HB} = 3.3, whereas we observed n_{HB} ranging from 2.6 for the small systems to 3.0 for the large systems.

Diffusion coefficients were calculated from mean square displacements and are given in Table 6. For zinc, experimentally derived self diffusion coefficients D_{Zn} between 0.14 [31] and 0.41 [32] and 0.49 [13] were reported. The latter two are in good agreement with our values in the range from 0.32 to 0.49. The first was calculated from NMR studies of highly concentrated (c = 17.2 M) solutions of $ZnCl_2$, where the high concentration might reduce the mobility of the solute. D_{Zn} was larger in the large systems (Zn-525, Zn-525-K) than in the smaller systems (Zn-123, Zn-123-K). This difference might be attributed to the strong hydration of zinc, which involves at least two hydration spheres as deduced from the RDF. Two hydration spheres with a total radius of approx. 6 Å consume most of the volume of the smaller systems (box length = 15.5 Å), reducing the number of free water molecules to a minimum and thus hindering the free diffusive motion of the solute as hypothesised above in the case of the highly concentrated $ZnCl_2$ solution.

For pure water, Weingärtner [33] gives an experimental value of D = 2.30. This is slightly lower than the values calculated from the simulations but these results are in good agreement with D = 2.67 reported for the SPC water model by Zhang et al. [34]. The reason for the increased mobility of water in the case of Zn-525-K is not known.

No exchange of a water molecule from the first hydration shell of zinc could be observed even during 1 ns of simulation time (Zn-123 and Zn-525). This stability of zinc's first hydration shell is not surprising: Laurenczy et al.[35] observed water exchange constants for Zn^{2+} of $0.3 \times 10^8\ s^{-1} < k_{ex}^{298} < 6 \times 10^8\ s^{-1}$ which is slower than the time scale of 1 ns covered by our longest simulations. Fratiello et al. [11] calculated an exchange rate of $10^8\ s^{-1}$, and Salmon et al. [13] estimated from QENS experiments a zinc to water-proton binding time between 10^{-10} s and 5×10^{-9} s. The latter is close to our simulation time. However, the exchange of protons is believed to occur faster than the exchange of com-

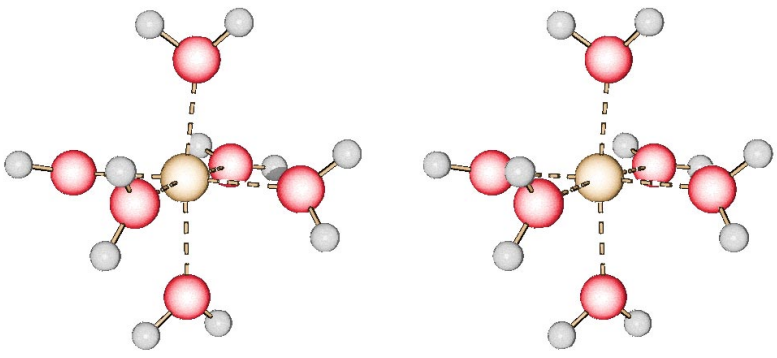

Figure 5. *Stereo plot of the first hydration shell of zinc. Representative snapshot from simulation Zn-123 chosen for its minimum deviation from the average hydration shell structure. White: hydrogen; red: oxygen; brown: zinc. The plot was generated using SCHAKAL (E. Keller, Freiburg).*

Table 6. *Diffusion coefficients for Zn^{2+} and water. D_{H_2O} (Zn): average diffusion coefficient of water (zinc) calculated from 50 intervals at 5 ps each; sd: standard deviation of D. From the calculation of D_{H_2O}, all molecules in the first hydration shell of zinc were excluded.*

System	D_{H_2O} ($10^{-5}cm^2/s$)	sd	D_{Zn} ($10^{-5}cm^2/s$)	sd
Zn-123	2.44	0.12	0.35	0.06
Zn-123-K	2.38	0.08	0.32	0.04
Zn-525	2.55	0.04	0.49	0.15
Zn-525-K	2.84	0.04	0.46	0.17
H_2O-125	2.50	0.03		

plete water molecules [14] and this proton transfer can not be observed by our conventional MD simulation.

Conclusion

Most of the parameters investigated are better reproduced by the CHARMM22 parameters than by the modified parameters published by Stote and Karplus. Especially the Zn-O distance of the former is in better agreement with experimental and theoretical results. Other properties like diffusion coefficients were not influenced by the parameter set but by the system size. Even simple systems like the ones investigated here require the use of systems larger than our small systems with 125 water molecules.

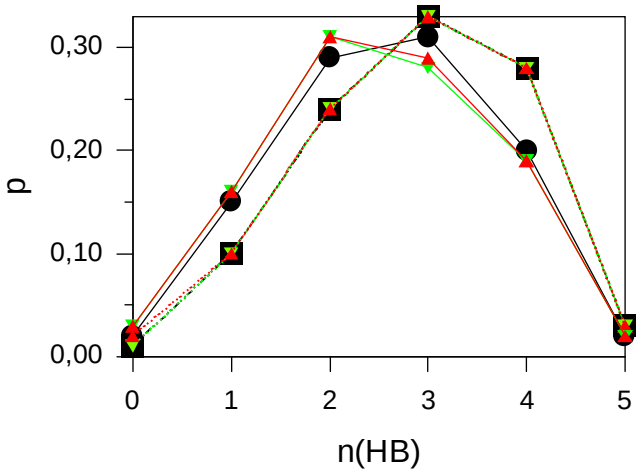

Figure 6. *Fraction p of water molecules participating in a given number of hydrogen bonds n(HB). Solid line: small system (15.5 Å)^3; dotted line: large system (25.08 Å)^3; red triangles: CHARMM22 parameters; green triangles: Stote/Karplus parameters; black dots: H_2O-125; black squares: H_2O-528.*

Supplementary material: 3D coordinates of the first hydration shell of zinc in PDB-format.

References

1. Christianson, D.W. *Adv. Protein Chem.* **1991**, *42*, 281.
2. Lipscomb, W.N.; Sträter, N. *Chem. Rev.* **1996**, *96*, 2375.
3. Bock, C.W.; Kaufman-Katz, A.; Glusker, J.P. *J. Am. Chem. Soc.* **1995**, *117*, 3754.
4. Paschina, G.; Piccaluga, G.; Pinna, G.; Magini, M. *J. Chem. Phys.* **1983**, *78*, 5745.
5. Licheri,G.; Paschina, G.; Piccaluga, G.; Pinna, G. *Z. Naturforsch.* **1982**, *37a*, 1205.
6. Dagnall, S.P.; Hague, D.N.; Towl, A.D.C. *J. Chem. Soc., Faraday Trans. 2* **1982**, *78*, 2161.
7. Powell, D.H.; Gullidge, P.M.N., Neilson, G.W.; Bellissent-Funel, M.C. *Mol. Phys.* **1990**, *71*, 1107.
8. Enderby, J.E. *Chem. Soc. Rev.* **1995**, *23*, 159.
9. Neilson, G.W.; Enderby, J.E. *Adv. Inorg. Chem.* **1989**, *34*, 195.
10. Lagarde, P.; Fontaine, A.; Raoux, D.; Sadoc, A.; Migliardo, P. *J. Chem. Phys.* **1980**, *72*, 3061.
11. Fratiello, A.; Kubo, V.; Peak, S.; Sanchez, B.; Schuster, R.E. *Inorg. Chem.* **1971**, *10*, 2552.
12. Caminiti, R.; Cucca, P.; Monduzzi, M.; Saba, G.; Crisponi, G. *J. Chem. Phys.* **1984**, *81*, 543.
13. Salmon, P.S.; Bellissent-Funel, M.C.; Herdman, G.J. *J. Phys.: Condens. Matter* **1990**, *2*, 4297.
14. Ohtaki, H.; Radnai, T. *Chem. Rev.* **1993**, *93*, 1157.
15. Marcus, Y. *Chem. Rev.* **1988**, *88*, 1475.
16. Johansson, G. *Adv. Inorg. Chem.* **1992**, *32*, 159.
17. Clementi, E.; Corongiu, G.; Jönsson, B.; Romano, S. *J. Chem. Phys.* **1980**, *72*, 260.
18. Yongyai, Y.P.; Kokpol, S.; Rode, B.M. *Chem. Phys.* **1991**, *156*, 403.
19. Marchese, F.T.; Beveridge, D.L. *Int. J. Quant. Chem.* **1986**, *29*, 619.
20. Stote, R.H.; Karplus, M. *Proteins* **1995**, *23*, 12.
21. Brooks, B. R.; Bruccoleri, R. E.; Olafson, B. D.; States, D. J.; Swaminathan, S.; Karplus, M. *J. Comput. Chem.* **1983**, *4*, 187.
22. Obst, S.; Bradaczek, H. *J. Phys. Chem.* **1996**, *100*, 15677.
23. Jorgensen, W.L.; Chandrashekhar, J; Madura, J.D.; Impey, R.W.; Klein, M.L. *J. Chem. Phys.* **1983**, *79*, 926.
24. van Gunsteren, W. F.; Berendsen, H. J. C. *Mol. Phys.* **1977**, *34*, 1311.
25. Allen M. P.; Tildesley, D. J. *Computer Simulation of Liquids*; Oxford University Press: Oxford, 1987; Chapter 1.
26. Garcia, A. E.; Stiller, L. *J. Comput. Chem.* **1993**, *14*, 1396.

27. Kowall, T.; Geiger, A. *J. Phys. Chem.* **1994**, *98*, 6216.
28. Einstein, A. *Ann. Phys.* **1905**, *17*, 549.
29. Powell, D.H.; Neilson, G.W. *J. Phys. Condens. Matter* **1990**, *2*, 3871.
30. Degrève, L.; de Pauli, V.M.; Duarte, M.A. *J. Chem. Phys.* **1997**, *106*, 655.
31. van der Maarel, J. *J. Magn. Reson.* **1989**, *81*, 92.
32. Bellissent-Funel, M.C.; Dianoux, A.J.; Fontana, M.P.; Maisona, G.; Migliardo, M. In *Water and aqueous solutions*; Neilson, G.W.; Enderby, J.E., Ed; A. Hilger: Bristol, 1986; p. 199.
33. Weingärtner, H. Z. *Phys. Chem. NF* **1982**, *132*, 129.
34. Zhang, L.; Ted Davis, H.; Kroll, D. M.; White, H. S. *J. Phys. Chem.* **1995**, *99*, 2878.
35. Laurenczy, G; Ducommun, Y.; Merbach, A.E. *Inorg. Chem.* **1989**, *28*, 3024.
36. Neilson, G.W.; Ansell, S.; Wilson, J. *Z. Naturforsch.* **1995**, *50a*, 247.
37. Ohtaki, H.; Yamaguchi, T.; Maeda, M. *Bull. Chem. Soc. Jpn.* **1976**, *49*, 701.